SELF-EXCITED OSCILLATIONS IN VARIABLE DENSITY COUNTER-CURRENT ROUND JETS

Karol Wawrzak
Department of Thermal Machinery
Czestochowa University of Technology
Al. Armii Krajowej 21, 42-201 Czestochowa, Poland
karol.wawrzak@pcz.pl

Andrzej Boguslawski
Department of Thermal Machinery
Czestochowa University of Technology
Al. Armii Krajowej 21, 42-201 Czestochowa, Poland
andrzej.boguslawski@pcz.pl

ABSTRACT

The paper focuses on a global instability phenomenon in variable density counter-current round jets. The analysis is performed using a large eddy simulation and the computations are carried out employing a high-order numerical code. The configuration of two co-axial nozzles, where suction applied in an annular nozzle is a driving force for the counterflow, is investigated for different velocity and density ratios. The research have shown the emergence of two global modes depending of the velocity and density ratios.

INTRODUCTION

Round jets have been studied theoretically, experimentally as well as numerically for decades. Their widespread presence in many industrial devices has inspired scientists to find a way to control them to obtain desired properties. One of the most interesting phenomena emerging in round jets, which considerably influences their behavior, is the self-excited global instability phenomenon triggered by absolutely unstable local flow regions (Huerre & Monkewitz, 1990). The theoretical predictions of Monkewitz & Sohn (1988) and Jendoubi & Strykowski (1994) showed that the absolute instability can be induced in variable density and counter-current jet configurations. Jendoubi & Strykowski (1994) identified two distinct absolutely unstable modes called Mode I and Mode II. The main features of the modes are: (i) Mode I has maximum fluctuation in the shear layer region, while Mode II has maximum on the jet centreline; (ii) both modes become more unstable as the velocity ratio $I = U_2/U_1$ (U_1 - velocity of the jet, U_2 - velocity of the counterflow) is increased, the density ratio $S = \rho_{jet}/\rho_{ambient}$ is decreased or the Mach number is decreased; (iii) Mode I is absolutely unstable only provided that $I > 0$ whereas Mode II does not require any counterflow below critical density ratio $S_{cr} \approx 0.7$.

The results of linear stability analysis were confirmed in experimental (Strykowski & Niccum, 1991; Strykowski & Wilcoxon, 1993; Kyle & Sreenivasan, 1993; Hallberg & Strykowski, 2006) and numerical works (Lesshafft *et al.*, 2006, 2007; Foysi *et al.*, 2010; Boguslawski *et al.*, 2016; Wawrzak
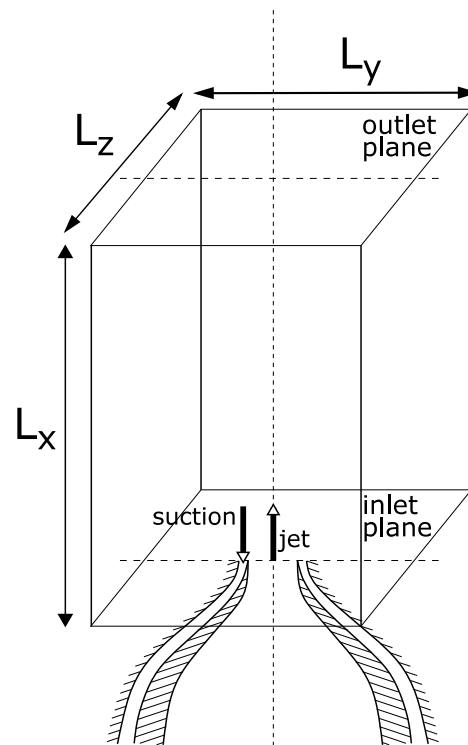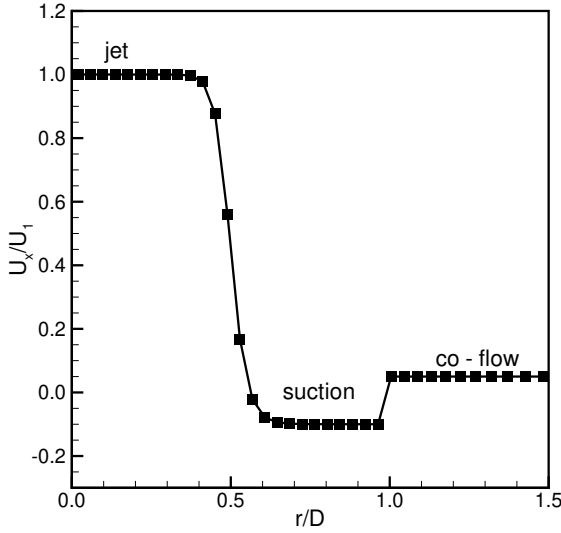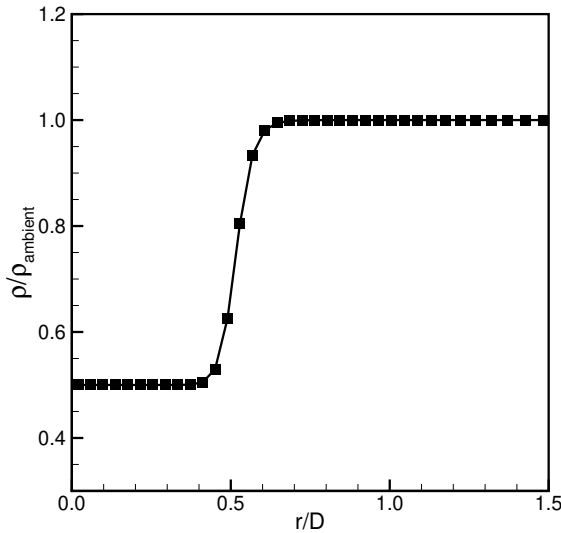
Figure 1. Schematic view on computational configuration.

et al., 2021). Despite the fact that the research cited above univocally showed the occurrence of the global instability in the counter-current jets, there is a lack of an analysis demonstrating a clear distinction between Mode I and Mode II in the available literature. Moreover, there are no investigations devoted to hot round jets with the counter-flow to the best authors' knowledge. The present paper is aimed at extending the knowledge concerning the global instability in variable density
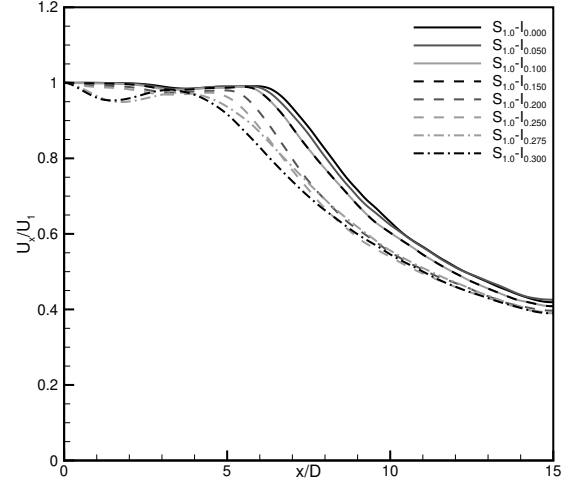
(a)

(b)

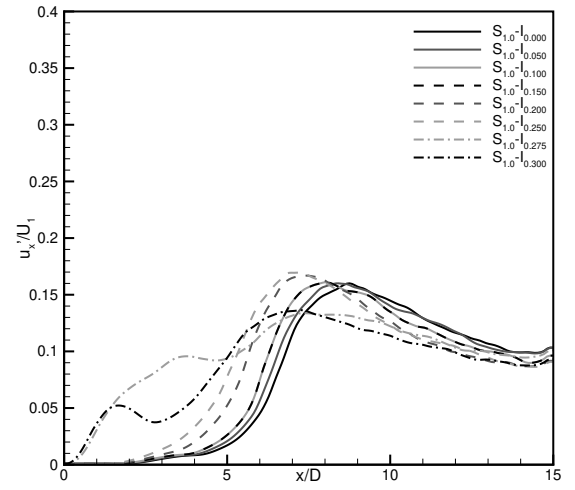Figure 2. Mean velocity (a) and density (b) profiles.

(a)

(b)

Figure 3. Time-averaged mean (a) and fluctuating (b) velocity profiles along the jet axis for $S = 1$.

jets by adding a counterflow.

NUMERICAL ALGORITHM AND COMPUTATIONAL PARAMETERS

We consider an incompressible variable density flow for which the filtered continuity and Navier-Stokes equations are solved using large eddy simulation (LES). The LES calculations are performed using an academic high-order solver SAILOR based on the low Mach number approximation. The code employed in this study was used previously in various computations including isothermal, non-isothermal, excited and reacting jets (Boguslawski *et al.*, 2017). A solution algorithm is based on a projection method for the pressure-velocity coupling. The time integration is performed by a predictor-corrector (Adams-Bashforth/Adams-Moulton) approach. The model equations are discretized in space using the 6th order compact difference method for half-staggered meshes (Tyliszczak, 2014; Tyliszczak A., 2016).The sub-grid

scales resulting from the LES filtering are modelled using the sub-grid model of Vreman (Vreman, 2004).

The calculations are performed for the configuration shown schematically in Fig. 1, which corresponds to the experimental configuration of Strykowski & Niccum (1991). In the present simulations, the internal geometry of the nozzles is not included in the computational domain. Instead, the jet is modeled through velocity and density profiles at the inlet plane. The computational domain is a simple rectangular box with dimensions $L_x = 15D, L_y = L_z = 6D$, where D is the diameter of the central main jet and x is the axial direction.

The inlet boundary conditions are specified in terms of the mean density and instantaneous velocity profiles. The inlet velocity profile is computed by adding fluctuating velocity components to the mean values. The velocity fluctuations are computed applying the digital filtering method proposed by Klein *et al.* (2003) whereas the inlet mean velocity is described by the hyperbolic-tangent profile. The inlet turbulence intensity is assumed at the level of $0.001U_1$. A low-velocity co-flow equal to $0.05U_1$ is added outside the jet region to mimic natural entrainment from the surroundings. The inlet density profile is obtained from the Busemann-Crocco relation (Schlichting & Gersten, 1979). The mean velocity and density profiles as-
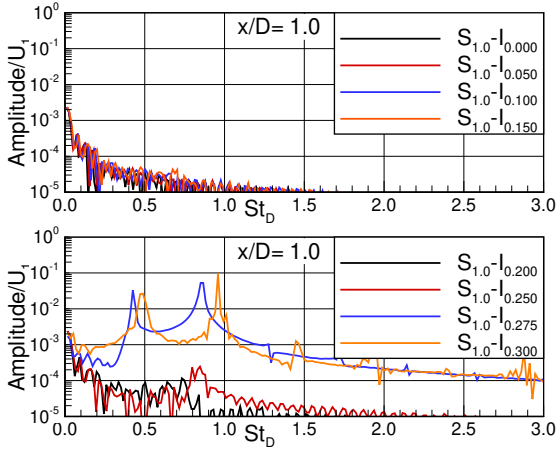
Figure 4. Evolution of the spectra of the axial velocity fluctuations registered at the jet axis for $S = 1$.

sumed at the inlet plane are presented in Fig. 2.

The Reynolds number defined as $Re_D = U_1 D/\nu$, where ν is the kinematic viscosity, is equal to $Re_D = 5000$. The analysis is performed for a jet with the shear layer thickness characterized by the parameter $D/\theta = 40$, various velocity ratios $I = 0 - 0.3$, and density ratios equal to $S = 0.5, 0.7, 1$. It should be noted that a relatively thick shear layer has been chosen to avoid interactions with the self-sustained convective oscillations reported by Boguslawski *et al.* (2013, 2019) that appear for $D/\theta > 50$.

The computations were carried out on the mesh consisting of $192 \times 128 \times 128$ points in x, y, z directions, respectively. Preliminary computations showed that such a mesh density is sufficient to obtain virtually grid independent results.

RESULTS

As mentioned above the analysis was performed for three density ratios. The first density ratio $S = 1$ corresponds to the homogeneous jet for which a counterflow ($I > 0$) is required to trigger both global modes. The next density ratio $S = 0.7$ is slightly above the critical density ratio S_{cr} below which global Mode II do not require any counterflow ($I = 0$) for a jet with shear layer characterized by $D/\theta = 40$. The last density ratio $S = 0.5$ is below critical S_{cr} for global Mode II without counterflow.

Figure 3 presents the profiles of the time-averaged axial mean and fluctuating velocity obtained for $S = 1$ and velocity ratio varying from $I = 0$ to 0.3. Note that the particular cases are hereafter denoted as $S_S - I_I$, e.g. $S_{1.0} - I_{0.10}$ refers to $S = 1.0$ and $I = 0.1$. It can be seen that the jets with $I = 0.0 - 0.15$ are characterised by the mean velocity profiles weakly dependent on I parameter. The profiles are nearly identical and characteristic for a circular free jet with the potential core length approximately equal to $5 - 6D$. Despite a more rapid decay of the mean velocity for $I = 0.2$ and $I = 0.25$, all the profiles are similar. A stronger impact of velocity ratio I on the mean profiles is observed for $I = 0.275$ and $I = 0.3$. Local minima at the axial distances $x/D \approx 2$ appear for both the cases. Changes of the mean velocity profiles are connected with alteration of the profiles of the velocity fluctuations. For $I = 0 - 0.25$ their shapes are similar and typical for round free jets. In these cases, the fluctuations start growing at $x/D \approx 3$ and achieve a level of 18% of U_1. A significant change is observed for the two last $I = 0.275, 0.3$, for which the growth of
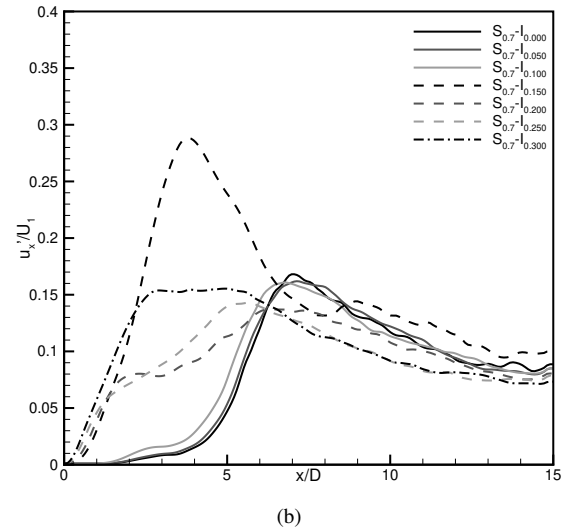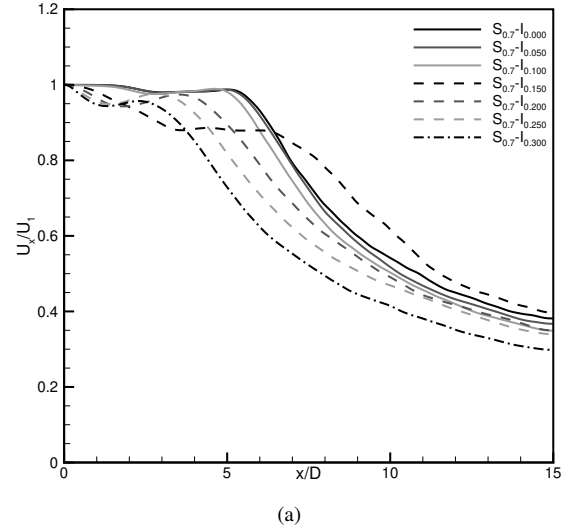

(a)

(b)

Figure 5. Time-averaged mean (a) and fluctuating (b) velocity profiles along the jet axis for $S = 0.7$.
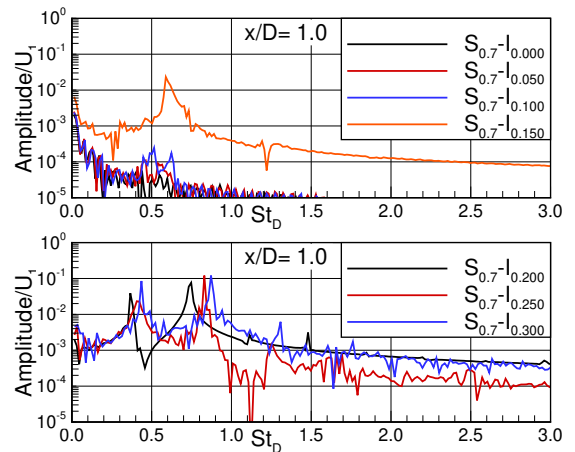

Figure 6. Evolution of the spectra of the axial velocity fluctuations registered at the jet axis for $S = 0.7$.

the fluctuations starts right from the nozzle exit. Additionally, for $I = 0.3$ the profile of fluctuations is characterised by the local maximum that correspond to the local minimum of the

(a)

Figure 8. Evolution of the spectra of the axial velocity fluctuations registered at the jet axis for $S = 0.5$.
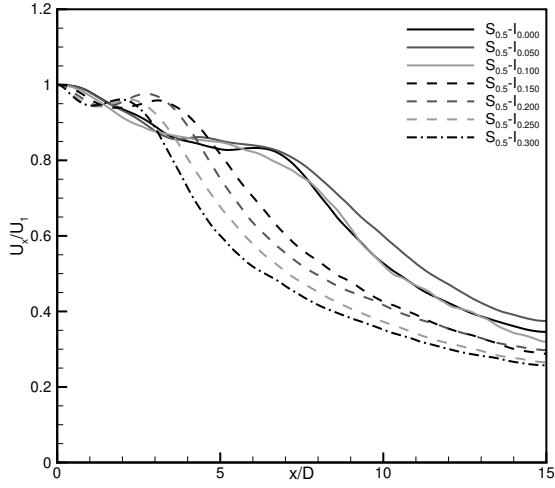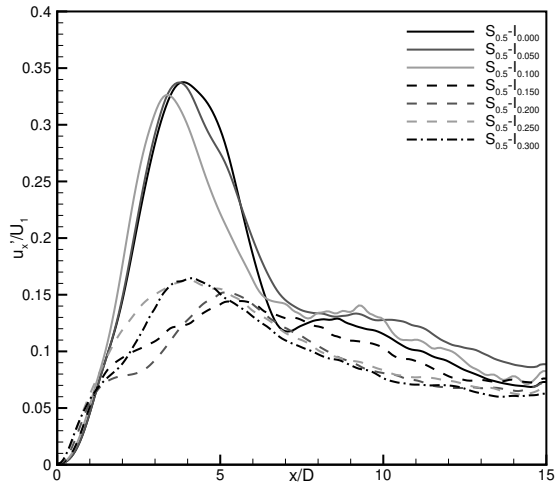
(b)

Figure 7. Time-averaged mean (a) and fluctuating (b) velocity profiles along the jet axis for $S = 0.5$.

mean velocity profile. Such profiles are characteristic for occurrence of the global Mode I in the jet flow as was presented by Strykowski & Niccum (1991) and Wawrzak *et al.* (2021). Therefore $I = 0.275$ can be considered as a critical velocity ratio I_{cr} for global Mode I for $S = 1$.

The emergence of the global oscillations is confirmed by Fig. 4 presenting the amplitude spectra of the axial velocity fluctuations registered at the axial location $x/D = 1.0$. The results obtained for the cases $S_{1.0} - I_{0.275}$ and $S_{1.0} - I_{0.30}$ reveal the existence of well-defined distinct peaks that indicate the formation of strong vortical structures. The peaks occur at $St_D = 0.85$ and 0.96 for the cases $S_{1.0} - I_{0.275}$ and $S_{1.0} - I_{0.30}$, respectively.

Figure 5 presents the profiles of the time-averaged axial mean and fluctuating velocity obtained for $S = 0.7$ and velocity ratio varying from $I = 0$ to 0.3. In this case, the sudden change in the time-averaged profiles is observed for a lower velocity ratio than in the case of $S = 1$, i.e. for $I = 0.15$. Hence, the $I = 0.15$ can be considered as a critical velocity ratio. However, the fluctuating velocity profile for the case $S_{0.7} - I_{0.15}$ qualitatively differ from those obtained for $S = 1$. The perturbation growth is observed close to the nozzle exit and the fluctuations reaches $30\%U_1$ at the axial distance $x/D \approx 4$. Such a
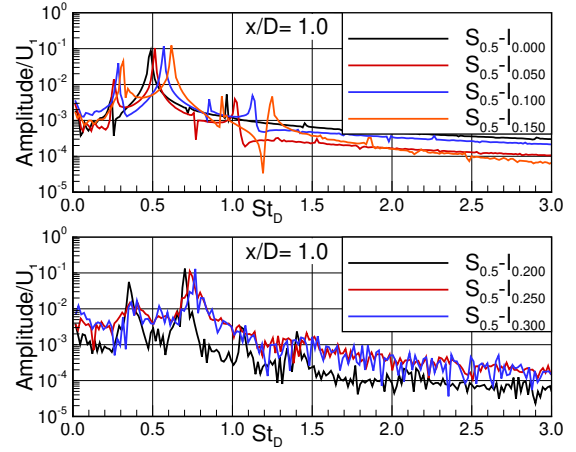
profile is characteristic for an emergence of global Mode II in the flow. For higher velocity ratios $I = 0.2, 0.25$ and $I = 0.3$ one can observe the damping of the fluctuations at the jet centerline which indicates a transition from global Mode II to global Mode I. It should be noted that $S = 0.7$ is only slightly above the critical density ratio below which global Mode II does not require any counterflow for the jet with $D/\theta = 40$. For $S = 0.7$ the velocity ratio $I = 0.15$ is a critical velocity ratio for global Mode II while the $I = 0.2$ is a critical velocity ratio for global Mode I. The obtained results are in good agreement with linear stability analysis that showed that an increase in velocity ratio I decreases the critical density ratio for both global modes.

Looking at the spectra presented in Fig. 6 one can observe that a decrease in the density ratio slightly lowers the non-dimensional frequency St_D in the case of global Mode I. Global Mode I is characterised by $St_D = 0.75, 0.81$ and 0.9 for $S_{0.7} - I_{0.2}$, $S_{0.7} - I_{0.25}$ and $S_{0.7} - I_{0.3}$. Such an observation is in good agreement with theoretical predictions of Jendoubi & Strykowski (1994). Regarding global Mode II ($S_{0.7} - I_{0.15}$) the frequency is lower than for Mode I and characterised by $St_D = 0.6$.

Figure 7 presents the profiles of the time-averaged axial mean and fluctuating velocity obtained for the last density ratio considered, i.e. $S = 0.5$. In this case, as expected, the global instability is observed for all the velocity ratios considered. As can be deduced from the velocity profiles both global modes appeared in the flow. For the cases $S_{0.5} - I_{0.0}$, $S_{0.5} - I_{0.05}$ and $S_{0.5} - I_{0.10}$ global Mode II is observed while starting from $I = 0.15$ there is a transition from Mode II to Mode I. The change of the S to the lower value again decreased the critical velocity ratio for both modes. Another important dependence is well seen in the evolution of spectra presented in Fig. 8, namely the decrease in density ratio lower the frequency of the mode. However, this dependence is rather weak. Taking into consideration the dependence of the frequency on the velocity ratio one can observe that for all the density ratio $S = 0.5, 0.7.1$ the increase in I parameter causes an increase in St_D value for both modes. A similar impact of density and velocity ratios on the frequency of the global modes was predicted by linear stability analysis (Jendoubi & Strykowski, 1994).

Figure 9 shows iso-surfaces of the Q-parameter and the axial velocity contours for both global modes. The Q-parameter is commonly used to indicate organised vortical structures and is defined as $Q = 1/2(|\Omega|^2 - |S|^2)$, where Ω
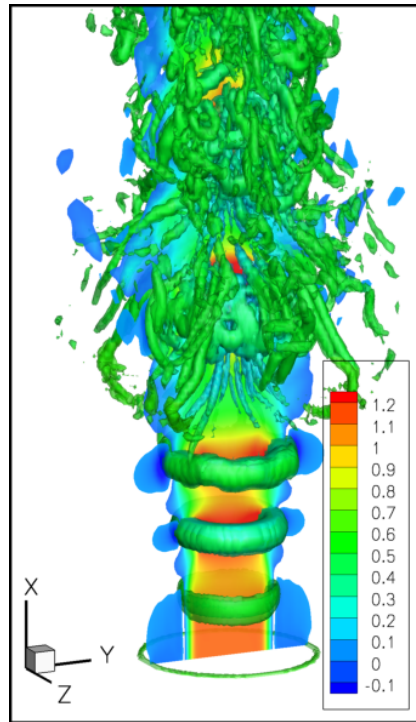
(a)
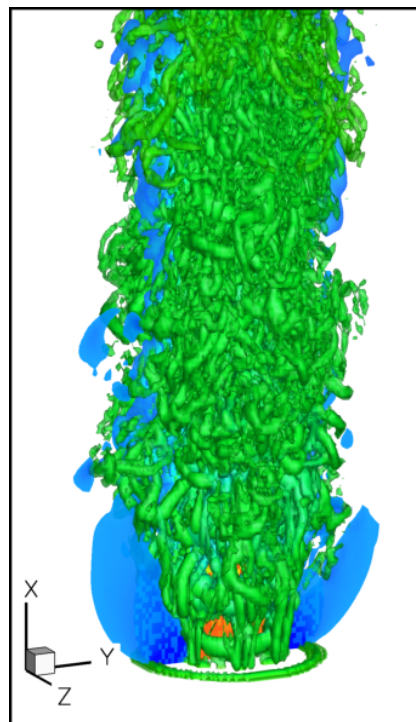
(b)

Figure 9. Iso-surfaces of instantaneous value of the Q-parameter with the axial velocity contours at the main cross-section for the cases: $S_{0.5} - I_{0.00}$ (a) and $S_{0.5} - I_{0.20}$ (b).

is the vorticity tensor and S is the rate of strain tensor. The case $S_{0.5} - I_{0.00}$, for which global Mode II is observed, is characterized by a formation of strong vortices close to the nozzle. They pair up and consequently break up further downstream. The formation of vortices even closer to the nozzle and a significantly faster break-up of the structures is observed for the second case presented in Fig. 9(b) for which the global Mode I

is identified. In this case, the mixing processes are drastically intensified already from the inlet plane. This may be desirable from a practical application point of view, e.g. in combustion chamber, where the fuel/oxidiser mixing is important.

CONCLUSION

The paper presents the LES study on counter-current variable density jets characterized by three density ratios: (i) $S = 1$ much above; (ii) $S = 0.7$ very close to; (iii) $S = 0.5$ below the critical value for which the global instability is triggered in the jet without the counterflow. Wide range of the velocity ratio I controlling the suction were considered that allow us to observe both globally unstable modes. Consistently to the literature, the critical velocity ratio for both modes decreases along with a decreae of the density ratio. Nevertheless, the variable density counter-current round jets still require significanlty deeper analysis.

ACKNOWLEDGEMENTS

REFERENCES

Boguslawski, A., Tyliszczak, A., Drobniak, S. & Asendrych, D. 2013 Self-sustained oscillations in a homogeneous-density round jet. *J. Turbul.* **14** (4), 25–52.

Boguslawski, A., Tyliszczak, A., Wawrzak, A. & Wawrzak, K. 2017 Numerical simulation of free jets. *Int . J. Numer. Meth. Heat Fluid* **27** (5), 1056–1063.

Boguslawski, A., Tyliszczak, A. & Wawrzak, K. 2016 Large eddy simulation predictions of absolutely unstable round hot jet. *Phys. Fluids* **28** (2), 025108.

Boguslawski, A., Wawrzak, K. & Tyliszczak, A. 2019 A new insight into understanding the crow and champagne preferred mode: a numerical study. *J. Fluid Mech.* **869**, 385–416.

Foysi, H., Mellado, J.P. & Sarkar, S. 2010 Large-eddy simulation of variable-density round and plane jets. *Int. J. Heat Fluid Flow* **31** (3), 307–314.

Hallberg, M.P. & Strykowski, P.J. 2006 On the universality of global modes in low-density axisymmetric jets. *J. Fluid Mech.* **569**, 493.

Huerre, P. & Monkewitz, P.A. 1990 Local and global instabilities in spatially developing flows. *Annu. Rev. Fluid Mech.* **22** (1), 473–537.

Jendoubi, S. & Strykowski, P.J. 1994 Absolute and convective instability of axisymmetric jets with external flow. *Phys. Fluids* **6** (9), 3000–3009.

Klein, M., Sadiki, A. & Janicka, J. 2003 A digital filter based generation of inflow data for spatially developing direct numerical or large eddy simulations. *J. Comput. Phys.* **186** (2), 652–665.

Kyle, D.M. & Sreenivasan, K.R. 1993 The instability and

breakdown of a round variable-density jet. *J. Fluid Mech.* **249**, 619–664.

Lesshafft, L., Huerre, P. & Sagaut, P. 2007 Frequency selection in globally unstable round jets. *Phys. Fluids* **19** (5), 054108.

Lesshafft, L., Huerre, P., Sagaut, P. & Terracol, M. 2006 Non-linear global modes in hot jets. *J. Fluid Mech.* **554**, 393–409.

Monkewitz, P.A. & Sohn, K. 1988 Absolute instability in hot jets. *AIAA J.* **26** (8), 911–916.

Schlichting, H & Gersten, K 1979 Boundary-layer theory new york: Macgraw hill.

Strykowski, P.J. & Niccum, D.L. 1991 The stability of countercurrent mixing layers in circular jets. *J. Fluid Mech.* **227**, 309–343.

Strykowski, P.J. & Wilcoxon, R.K. 1993 Mixing enhancement due to global oscillations in jets with annular counterflow. *AIAA J.* **31** (3), 564–570.

Tyliszczak, A. 2014 A high-order compact difference algorithm for half-staggered grids for laminar and turbulent incompressible flows. *J. Comput. Phys.* **276**, 438–467.

Tyliszczak A. 2016 High-order compact difference algorithm on half-staggered meshes for low Mach number flows. *Comput. Fluids* **127**, 131–145.

Vreman, A.W. 2004 An eddy-viscosity subgrid-scale model for turbulent shear flow: Algebraic theory and applications. *Phys. Fluids* **16** (10), 3670–3681.

Wawrzak, K., Boguslawski, A. & Tyliszczak, A. 2021 A numerical study of the global instability in counter-current homogeneous density incompressible round jets. *Flow Turbul. Combust.* pp. 1–35.